

## EXPERIMENTAL STUDY

# Rutaecarpine ameliorates cardiomyocyte injury induced by high glucose by promoting TRPV1-mediated autophagy

Chunhui SONG<sup>1</sup>, Zhigang GONG<sup>2</sup>, Yunxi JI

The First Clinical Medical College of Zhejiang Chinese Medicine University, Hangzhou, China.  
jiyunxi040@163.com

**ABSTRACT**

**AIM:** Diabetic cardiomyopathy (DCM) is a dominant factor contributing to diabetic death. Rutaecarpine has many cardiovascular biological effects and anti-high-glucose activity. Therefore, this paper aimed to investigate the impact of rutaecarpine on high glucose (HG)-elicited cardiomyocyte injury.

**METHOD:** Cell counting kit 8 (CCK-8) and 5-ethynyl-2'-deoxyuridine (EdU), TdT-mediated dUTP Nick-End Labeling (TUNEL) assays judged H9c2 cell activity and apoptosis, and oxidative stress was assessed by corresponding assay kits. The expression of apoptosis, oxidative stress, autophagy-associated factors and TRPV1 were examined with western blot. IF assay tested GFP-LC3 expression.

**RESULTS:** As a result, rutaecarpine had no obvious effect on the viability of H9c2 cells while elevated HG-exposed H9c2 cell viability. Rutaecarpine inhibited the apoptosis and oxidative stress of H9c2 cells induced by HG. In addition, rutaecarpine activated TRPV1 to induce autophagy. However, inhibition of TRPV1 inactivated the autophagy, which drove HG-evoked H9c2 apoptosis and oxidative stress.

**CONCLUSIONS:** In conclusion, rutaecarpine suppressed HG-stimulated H9c2 cell viability injury, apoptosis as well as oxidative stress via promoting TRPV1-mediated autophagy (Fig. 6, Ref. 40). Text in PDF [www.elis.sk](http://www.elis.sk)

**KEY WORDS:** rutaecarpine, TRPV1, autophagy, cardiomyocyte injury, high glucose.

**Introduction**

Diabetes mellitus is a common chronic disease with high morbidity and mortality (1). Diabetes can cause cardiomyopathy and increase the risk of heart failure unrelated to high blood pressure and coronary heart disease, known as diabetic cardiomyopathy (DCM) (2). The etiology of DCM is multifactorial. Insulin resistance and hyperglycemia are generally considered to be the main promoting factors of DCM (3). DCM has adverse prognostic effects in affected patients and there is currently no targeted therapy.

Rutaecarpine (Fig. 1A) is a pentacyclic indole quinoline alkaloid extracted from the nearly mature fruit of 'Wu-Chu-Yu' (4). Rutaecarpine exerts wide functions in cardiac events (5, 6). It has been reported that rutaecarpine can prevent hypertensive cardiac hypertrophy (7) and alleviate hypoxia-induced right ventricular remodeling in rats (8). In addition, rutaecarpine has been demonstrated to have anti-high-glucose activity and anti-diabetes activity. Studies have shown that rutaecarpine prevents endothelial cell senescence induced by high glucose through transient receptor

potential vanilloid 1/ sirtuin-1 (TRPV1/SIRT1) pathway (9) and enhances metformin's anti-diabetes activity by upregulating Oct1 in diabetic rats (10). Nonetheless, whether rutaecarpine functions in DCM demand prompt solution.

As a member of the superfamily of TRP channels, transient receptor potential vanilloid 1 (TRPV1) is a non-selective cation channel widely distributed in cell membrane and organelle membrane, and has good permeability for Ca<sup>2+</sup> and H<sup>+</sup> (11, 12). The activation of TRPV1/[Ca<sup>2+</sup>]<sub>i</sub>/CaM signaling can be stimulated by Rutaecarpine (10). TRPV1 activation induces autophagy to reduce the hypoxic injury of mouse myocardial cells (13). TRPV1 mediated autophagy could also regulate cell apoptosis and oxidative stress. The dissociation of TRPV1 suppressed autophagy-induced NLRP3 inflammasome activation and apoptosis (14). Oxidative stress-induced apoptosis could be inhibited by autophagy which was activated by TRPV1 in microglia (15).

Therefore, this paper aimed to investigate the impact of rutaecarpine on high glucose (HG)-elicited cardiomyocyte apoptosis and oxidative stress through the regulation of TRPV1 induced autophagy.

**Material and methods***Cell culture and treatment*

The rat myocardium-derived cell line H9c2 was provided from American Type Culture Collection (ATCC, USA). H9c2 cells were

<sup>1</sup>College of Life Sciences, Jiangxi Normal University, Nanchang, China,

<sup>2</sup>Physical Education College of Jiangxi Normal University, Nanchang, China, and <sup>3</sup>The First Clinical Medical College of Zhejiang Chinese Medicine University, Hangzhou, China

**Address for correspondence:** Yunxi JI, The First Clinical Medical College of Zhejiang Chinese Medicine University, No. 45 Post and Telecommunications Road, Hangzhou, 330000, China.

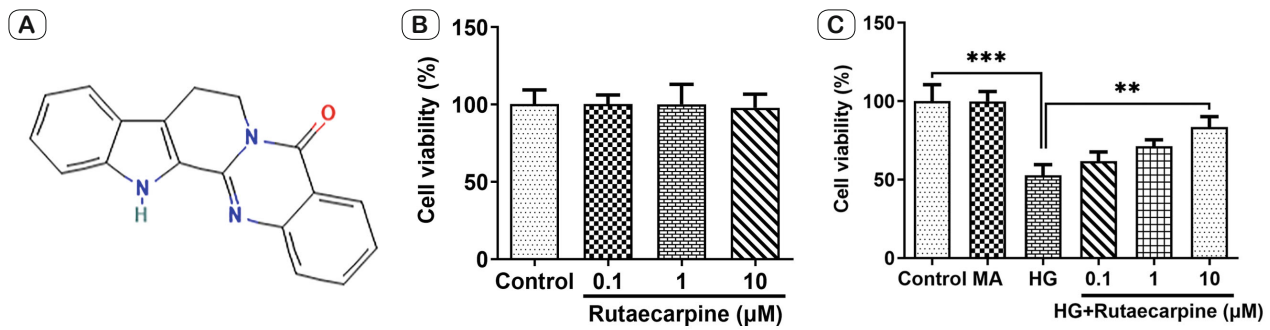


**Fig. 1.** Rutaeacarpine enhances H9c2 cell viability induced by HG. (A) The chemical structure of rutaeacarpine. (B) The viability of H9c2 cells treated by rutaeacarpine was detected by CCK-8 assay. (C) The viability of HG-induced H9c2 cells treated by rutaeacarpine was detected by CCK-8 assay. \*\*  $p < 0.01$  and \*\*\*  $p < 0.001$ .  $n = 3$ .

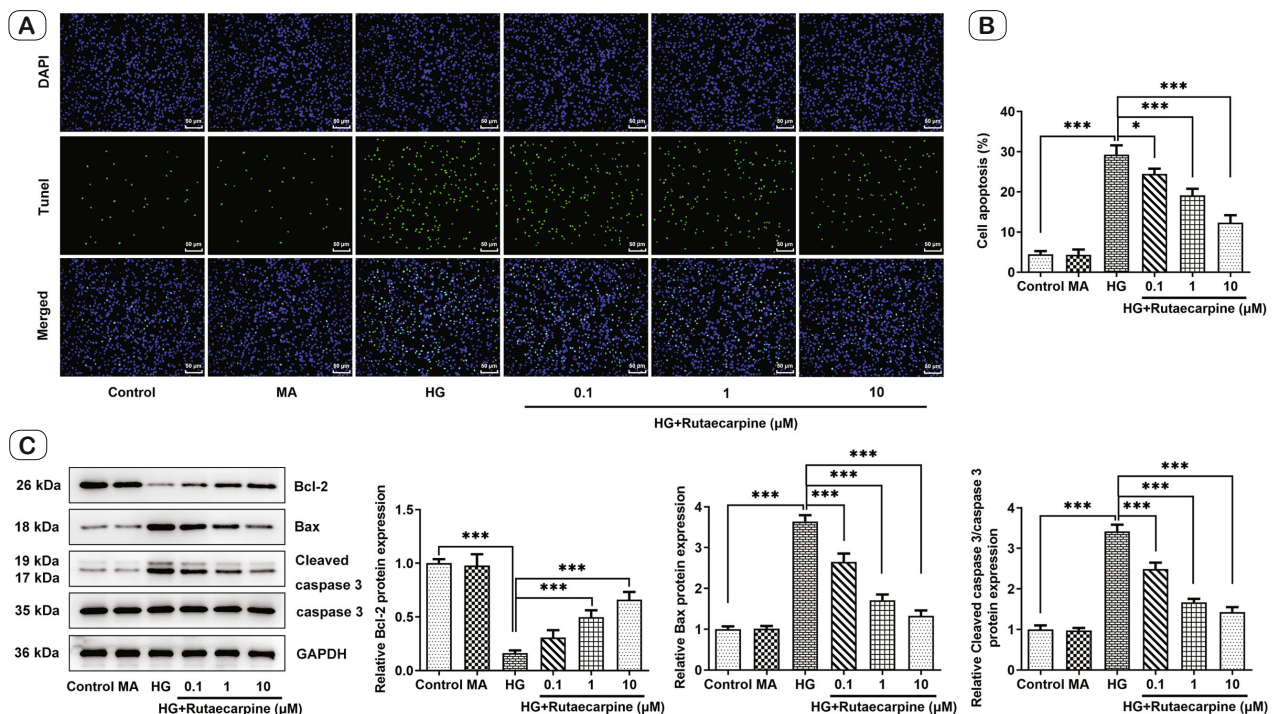


**Fig. 2.** Rutaeacarpine inhibits H9c2 cell apoptosis induced by HG. (A and B) The apoptosis of HG-induced H9c2 cells treated by rutaeacarpine was detected by TUNEL assay. (C) The expression of apoptosis-related proteins in HG-induced H9c2 cells treated by rutaeacarpine was analyzed by western blot. \*  $p < 0.05$  and \*\*\*  $p < 0.001$ .  $n = 3$ .

cultured in dulbecco’s modified eagle medium (DMEM; Gibco) containing 5.5 mmol/L d-glucose, 10 % fetal bovine serum (FBS), 100 U/ml penicillin, and 100 mg/ml streptomycin at 37 °C with 5 % CO<sub>2</sub>. The subsequent experiments were performed when the cell density reached about 80 %. In the cell toxicity test, H9c2 cells were treated with different concentrations of rutaeacarpine (0.1, 1, and 10 μM) for 1 h (16); In the HG-treated group, H9c2 cells were incubated with DMEM containing 33 mmol/L glucose for 24 h; In the MA-treated group, H9c2 cells were incubated with DMEM containing 33 mmol/L mannitol for 24 h; In the HG+rutaeacarpine group, H9c2 cells were pre-treated with different concentrations

of rutaeacarpine (0.1, 1, and 10 μM) 1 h prior to HG induction. In the HG+rutaeacarpine+TRPV1 inhibitor group, TRPV1 inhibitor AMG9810 (Tocris, Bristol, UK) was applied.

*Cell counting kit 8 (CCK-8) assay*

The CCK-8 kit (Beyotime) was used to measure the viability of H9c2 cells. H9c2 cells were seeded into the 96-well plates at 5000 cells/well and cultured at 37 °C. After treatment, H9c2 cells were added with 10 μL CCK8 solution at 24 h, which was then incubated for 2 h at 37 °C. The optical density values at a wavelength of 450 nm were detected using a microplate reader.

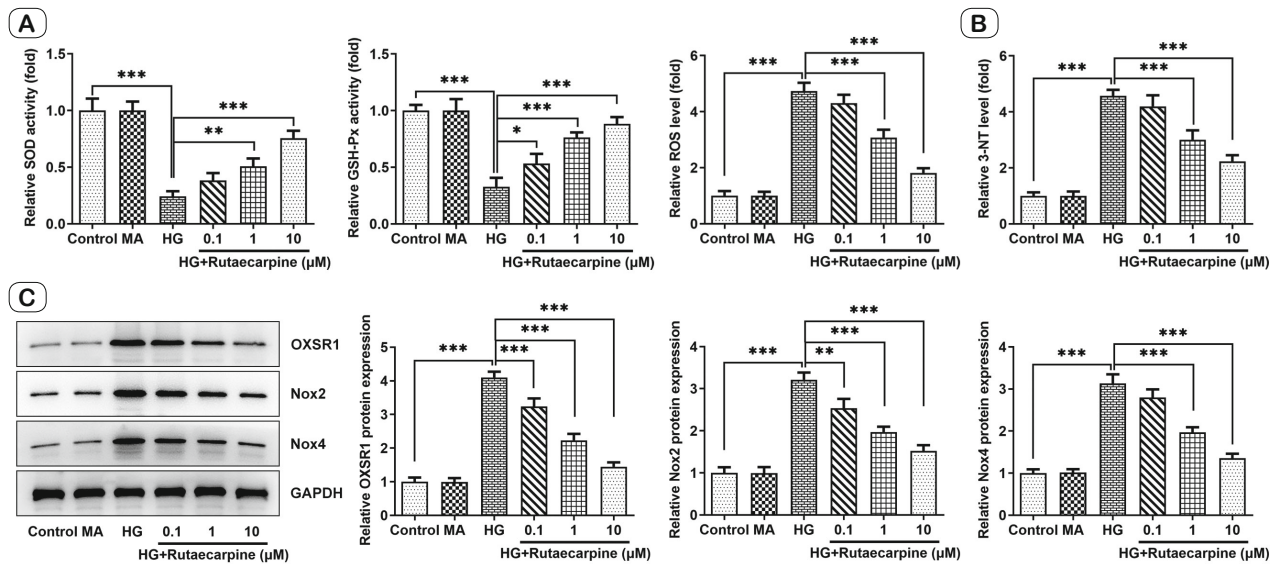


**Fig. 3. Rutaecarpine reduces H9c2 cell oxidative stress induced by HG.** (A) The SOD, GSH-Px activity and ROS, (B) 3-NT levels in HG-induced H9c2 cells treated by rutaecarpine were determined by their corresponding assay kits. (C) The expression of oxidative stress-related proteins in HG-induced H9c2 cells treated by rutaecarpine was analyzed by western blot. \*  $p < 0.05$ , \*\*  $p < 0.01$  and \*\*\*  $p < 0.001$ .  $n = 3$ .

*5-ethynyl-2'-deoxyuridine (EdU), TdT-mediated dUTP Nick-End Labeling (TUNEL)*

After treatment, H9c2 cells were first immobilized in 1% formaldehyde on ice for 15 min and mixed with 0.2% Triton X-100. Thereafter, cells were treated with fluorescein 2'-Deoxyuridine 5'-Triphosphate (dUTP)-end labeling for 60 min at 37 °C and cell nucleus was stained with DAPI staining solution (10 mM) for 5 min. Finally, cell apoptosis was observed by use of fluorescence microscope (Olympus Corporation) and quantified with ImageJ 1.8.0 software. Green dots showed positive cells with TUNEL staining (apoptotic cells).

*Western blot*

After treatment, proteins in H9c2 cells were harvested using radioimmunoprecipitation assay (RIPA) lysis buffer (Beyotime) with addition of protease inhibitors (Roche). The protein concentration was quantified by the BCA Protein Assay kit (Pierce; Thermo Fisher Scientific). Total proteins (30 μg) were separated by sodium dodecyl sulfate-polyacrylamide gel electrophoresis (SDS-PAGE) and transferred to a polyvinylidene difluoride (PVDF) membrane. Then, PVDF membranes were blocked with 5% BSA at room temperature for 1 h and incubated with primary antibodies against Bcl-2, Bax, Cleaved caspase 3, oxidative stress-responsive 1 (OXSR1), NADPH oxidases 2 (Nox2), Nox4, TRPV1, LC3-I, LC3-II, Beclin-1, p62 and GAPDH at 4 °C overnight. Secondary antibodies labeled by horseradish peroxidase were then used to culture the PVDF membrane at room temperature for 1 h. The protein bands were detected with an enhanced chemiluminescence kit (Thermo Fisher Scientific, Inc.) and were quantified through ImageJ 1.8.0 software.

*Detection of oxidative stress factors*

After treatment, H9c2 cells were washed with pre-cooling phosphate buffer saline (PBS) for two times and processed with pre-cooling PBS by homogenizer at 4 °C. Then, the homogenate was centrifuged at 4 °C and the supernatant was taken as the sample to be tested. The levels of superoxide dismutase (SOD), glutathione peroxidase (GSH-Px), reactive oxygen species (ROS) and 3-Nitrotyrosine (3-NT) in the supernatant were evaluated using their assay kits in accordance with the manufacturer's protocol.

*Immunofluorescence*

After treatment, H9c2 cells were fixed with 4% paraformaldehyde at 4 °C for 1 h and were permeabilized with 0.5% Triton X-100 for 20 min at room temperature. Then, cells were blocked with 5% bovine serum albumin (BSA) at 4 °C for 30 min and incubated with LC3 primary antibody at 4 °C overnight. After incubating with FITC-conjugated goat antibody for 1 h at room temperature, cells were stained with 4',6-diamidino-2-phenylindole (DAPI) for 5 min away from the light. The representative images were gathered using a fluorescence microscope (Olympus Corporation).

*Statistical analysis*

Data were presented as the mean ± SD from three independent experiments and were statistically analyzed by the software GraphPad Prism 8.0 (GraphPad Software, inc.). Differences among multiple groups were evaluated using ANOVA followed by Tukey's post hoc test. Statistical significance was considered as  $p < 0.05$ .

**Results**

*Rutaecarpine enhances H9c2 cell viability induced by HG*

The chemical structure of rutaecarpine was shown as Fig. 1A. The effect of rutaecarpine on viability of H9c2 cells with or without HG induction was assayed by CCK-8 assay. The viability of H9c2 cells was not significantly affected by the different concentrations of rutaecarpine (Fig. 1B). The induction of HG led to the decreased viability of H9c2 cells, which was improved by rutaecarpine at 10  $\mu$ M (Fig. 1C).

*Rutaecarpine inhibits H9c2 cell apoptosis induced by HG*

The effect of rutaecarpine on apoptosis of HG-induced H9c2 cells was determined by TUNEL assay and the apoptosis-related proteins expression was detected by western blot. The apoptosis of H9c2 cells was aggravated by the induction of HG and rutaecarpine gradually reduced the apoptosis of HG-induced H9c2 cells from 0.1 to 10  $\mu$ M (Figs 2A and B). The expression of Bcl-2 was downregulated and the expression of Bax and Cleaved caspase 3/caspase 3 was upregulated in H9c2 cells of HG group, which gradually reversed the effect of HG on the expression of apoptosis-proteins by rutaecarpine from 0.1 to 10  $\mu$ M (Fig. 2C).

*Rutaecarpine reduces H9c2 cell oxidative stress induced by HG*

The levels of oxidative stress-related indicators were detected by ELISA kits and the expression of oxidative stress-related proteins was analyzed by western blot. The levels of SOD and GSH-Px were suppressed and the levels of ROS and 3-Nitrotyrosine (3-NT) was promoted by HG in H9c2 cells (Figs 3A and B). The expression of OXSR1, Nox2 and Nox4 in HG-induced H9c2 cells was increased (Fig. 3C). The effects of HG on the above expression of oxidative stress factors and proteins could be reversed by rutaecarpine.

*Rutaecarpine activates TRPV1 to induce autophagy*

To investigate whether rutaecarpine could activate TRPV1 to induce autophagy, the expression of TRPV1 and autophagy-related proteins was determined by western blot and LC3 expression was showed by IF. HG inhibited the TRPV1 expression while rutaecarpine promoted the TRPV1 expression in HG-induced H9c2 cells (Fig. 4A). The expression of LC3-II/I and Beclin-1 was decreased while expression of p62 was increased in HG-induced H9c2 cells, which were all reversed by rutaecarpine (Fig. 4B). The result of immunofluorescence also indicated that LC3 expression was suppressed by HG and was enhanced by rutaecarpine in HG-induced

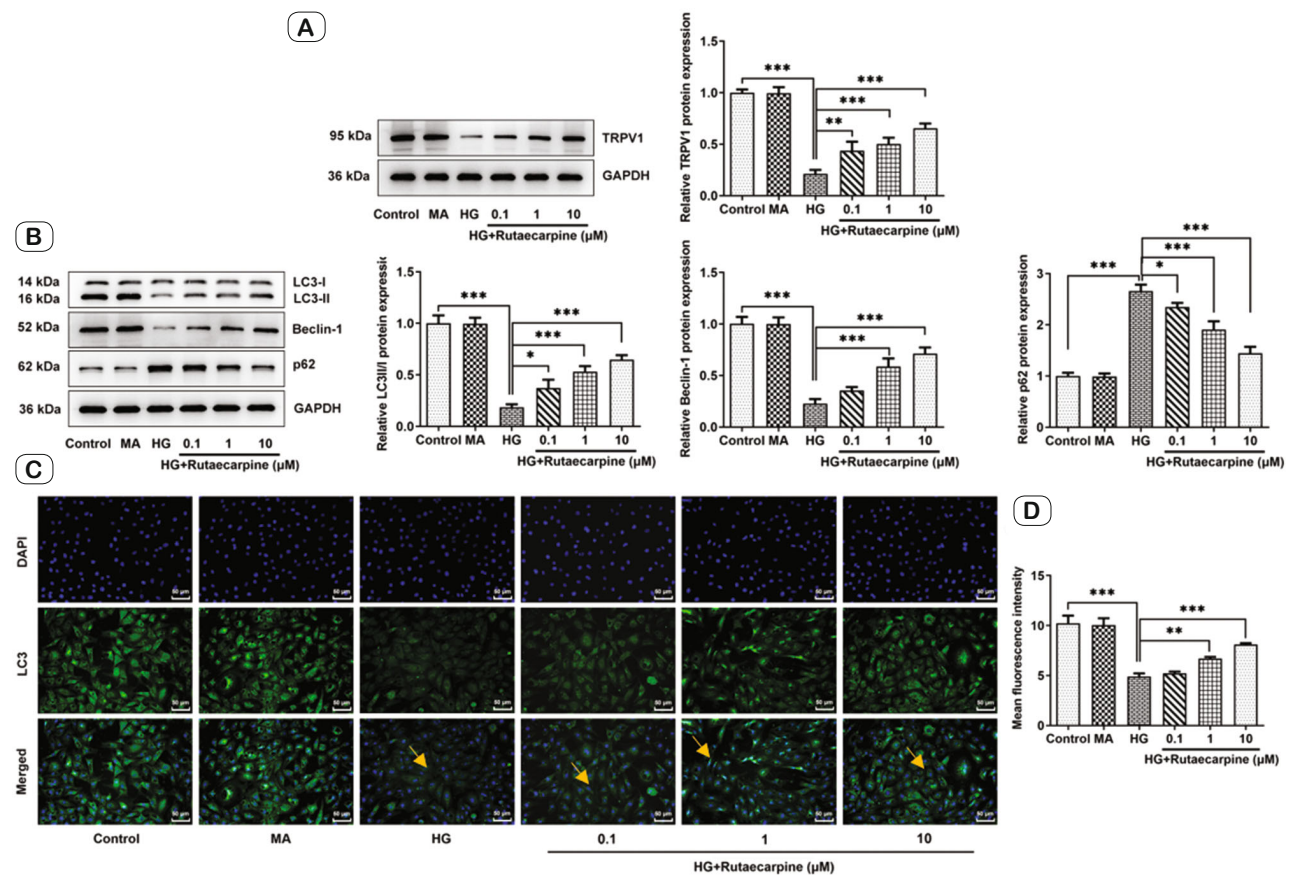


**Fig. 4.** Rutaecarpine activates TRPV1 to induce autophagy. (A) The TRPV1 expression in HG-induced H9c2 cells treated by rutaecarpine was detected by western blot. (B) The expression of autophagy-related proteins in HG-induced H9c2 cells treated by rutaecarpine was analyzed by western blot. (C and D) The expression of LC3 in HG-induced H9c2 cells treated by rutaecarpine was showed by immunofluorescence. \*  $p < 0.05$ , \*\*  $p < 0.01$  and \*\*\*  $p < 0.001$ .  $n = 3$ .

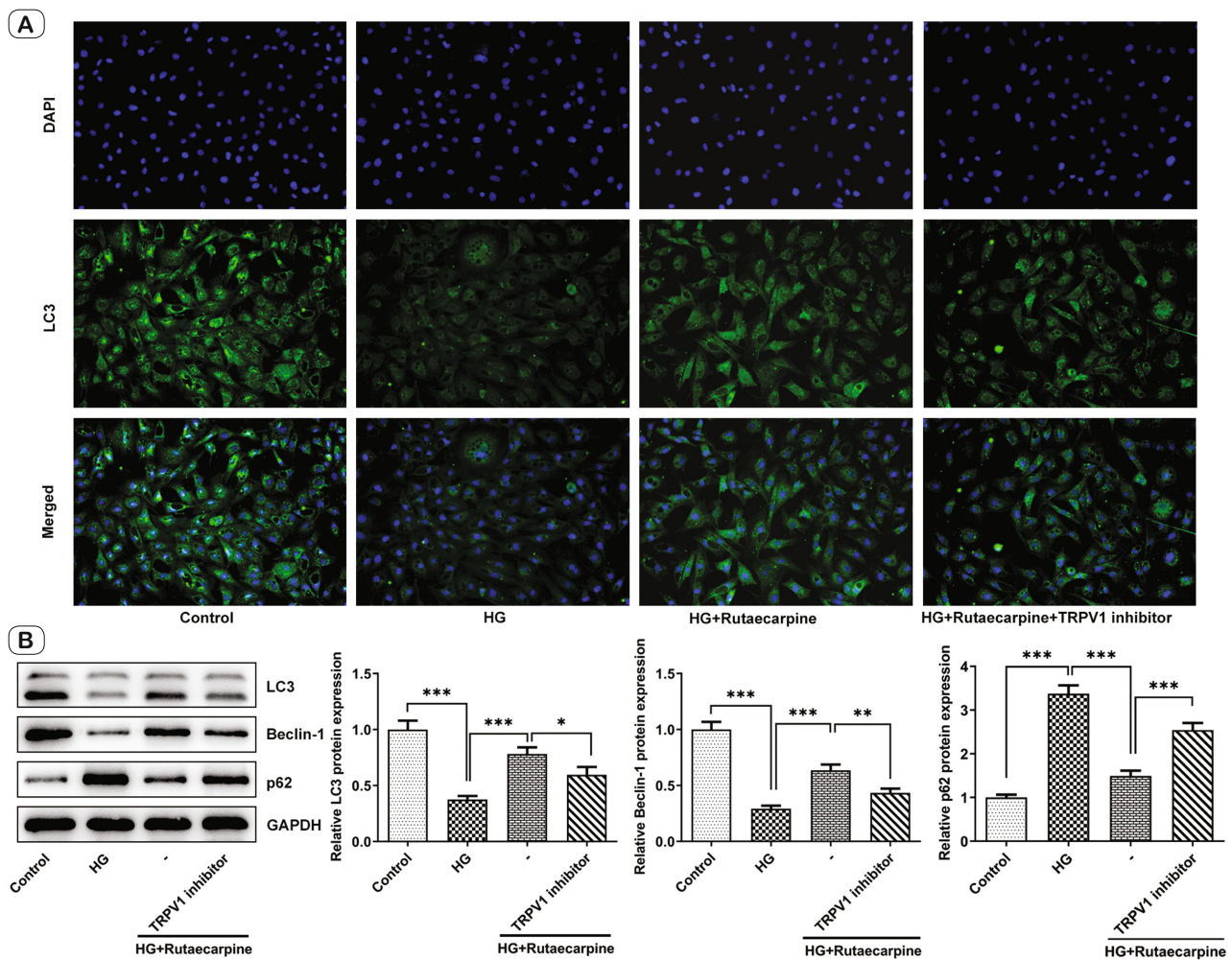


**Fig. 5.** Inhibition of TRPV1 reverses the impacts of rutaecarpine on the autophagy of HG-exposed H9c2 cells. (A) The expression of LC3 in HG-exposed H9c2 cells treated with rutaecarpine and TRPV1 inhibitor was showed by immunofluorescence. (B) The expression of autophagy-related proteins in HG-exposed H9c2 cells treated with rutaecarpine and TRPV1 inhibitor was analyzed by western blot. \*  $p < 0.05$ , \*\*  $p < 0.01$  and \*\*\*  $p < 0.001$ .  $n = 3$ .

H9c2 cells (Figs 4C–D). Therefore, the above results indicated that 10  $\mu\text{M}$  rutaecarpine was chosen for the subsequent study.

*Inhibition of TRPV1 reverses the impacts of rutaecarpine on the autophagy of HG-exposed H9c2 cells.*

To corroborate whether rutaecarpine elicited the protective role in HG-treated H9c2 cells via mediating TRPV1, TRPV1 inhibitor was applied. Subsequently, LC3 expression was showed by IF and the expression of autophagy-related proteins was determined by western blot. Immunofluorescence analysis showed that rutaecarpine elevated the decreased LC3 expression caused by HG exposure and TRPV1 inhibitor further declined the expression of LC3 in H9c2 cells treated with HG and rutaecarpine (Fig. 5A). The decreased LC3-II/I, Beclin-1 expression and increased p62 expression in HG-induced H9c2 cells were all restored by rutaecarpine. The Inhibition of TRPV1 suppressed the expression of LC3-II/I

and Beclin-1 and promoted the expression of p62 in H9c2 cells treated with HG and rutaecarpine again (Fig. 5B).

*Inhibition of TRPV1 reverses the effects of rutaecarpine on the apoptosis and oxidative stress in HG-exposed H9c2 cells*

Concurrently, the levels of apoptosis and oxidative stress were detected by TUNEL assay, ELISA kits and western blot. Inhibition of TRPV1 increased the apoptosis of H9c2 cells treated with HG and rutaecarpine (Fig. 6A), and downregulated the expression of Bcl-2 while upregulated the expression of Bax and Cleaved caspase 3/caspase 3 (Fig. 6B). The levels of SOD and GSH-Px were reduced and the levels of ROS and 3-NT was raised by the inhibition of TRPV1 in H9c2 cells treated with HG and rutaecarpine (Figs 6C–D). The expression of OXSR1, Nox2 and Nox4 was increased by the inhibition of TRPV1 in H9c2 cells treated with HG and rutaecarpine (Fig. 6E).

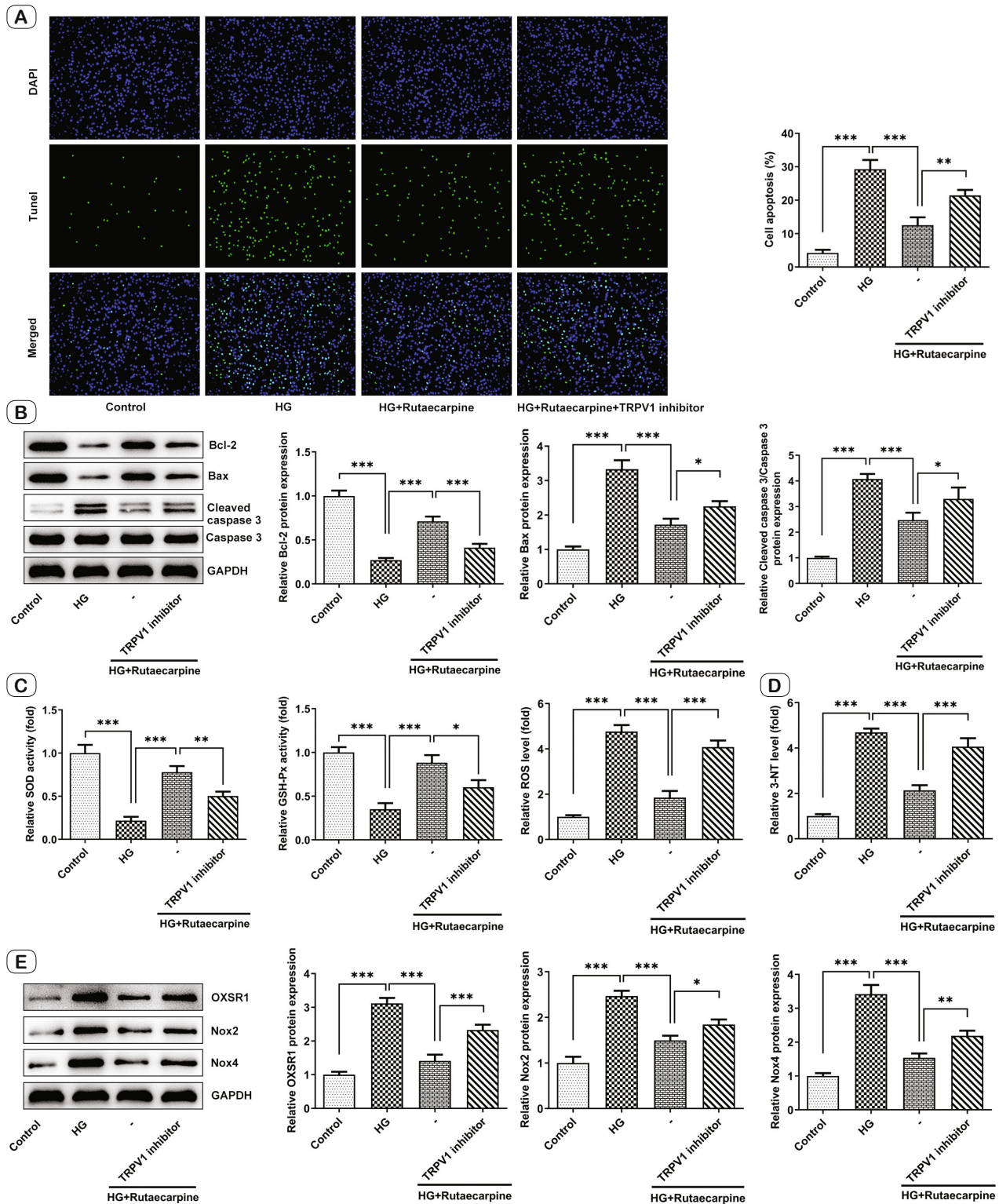


**Fig. 6.** Inhibition of TRPV1 reverses the protective effect of rutaecarpine on HG-induced H9c2 cells. (A) The apoptosis of HG-exposed H9c2 cells treated with rutaecarpine and TRPV1 inhibitor was detected by TUNEL assay. (B) The expression of apoptosis-related proteins in HG-exposed H9c2 cells treated with rutaecarpine and TRPV1 inhibitor was analyzed by western blot. (C) The SOD, GSH-Px activity and ROS, (D) 3-NT levels in HG-exposed H9c2 cells treated with rutaecarpine and TRPV1 inhibitor were determined by their corresponding assay kits. (E) The expression of autophagy related proteins in HG-exposed H9c2 cells treated with rutaecarpine and TRPV1 inhibitor was analyzed by western blot. \*  $p < 0.05$ , \*\*  $p < 0.01$  and \*\*\*  $p < 0.001$ .  $n = 3$ .

## Discussion

Studies indicated that rutaecarpine inhibited NADPH oxidase to prevent myocardial apoptosis induced by hypoxia and reoxygenation (16) and reversed isoproterenol-induced cardiac remodeling by stimulating calcitonin gene-related peptide production (17). In addition, rutaecarpine showed anti-diabetes potential in type 2 diabetic mice by regulating liver glucose homeostasis (18). Here, it was observed that rutaecarpine could improve HG-exposed H9c2 cell viability.

Currently known etiology of DCM includes inflammatory response, oxidative stress, mitochondrial dysfunction, programmed cell death, as well as myocardial fibrosis (19). It is reported that oxidative stress and inflammatory response play a major role in myocardial injury in DCM (20). Myocardial cells or tissues of diabetic cardiomyopathy mice can release a large amount of ROS, resulting in extracellular collagen deposition and increased cellular interstitial composition, promoting hyperplasia of connective tissues (21). SOD is a pivotal enzyme capable of defending against oxidative stress *in vivo*, which can reduce the formation of lipid peroxides and protect biofilm and biomolecular structure (22). In DCM mice, SOD activity decreased and ROS release increased, while EGCG could inhibit ROS release and increase SOD activity in myocardial tissue (23). The current study also clarified that rutaecarpine could relieve the oxidative stress induced by HG in H9c2 cells.

Studies on animal models of DCM showed that autophagy was inhibited at DCM, suggesting that the suppression of autophagy may be engaged in DCM (24, 25). It was found that at the early stage of DCM, activated autophagy could relieve insulin resistance and reduce oxidative stress to ameliorate myocardial metabolic disorder and oxygen deficiency (26). Gao WB et al. pointed out that the up-regulation of autophagy related protein expression level can enhance the autophagy activity of cardiomyocytes, reduce the death of cardiomyocytes and enhance cell survival to a certain extent, and thus play a protective role of cardiomyocytes (27). LC3 and Beclin1 are autophagy related genes in mammals, which play a key role in autophagy and can be used as markers of autophagy (28). This study indicated that autophagy-associated proteins (LC3-II/I and Beclin-1) expression were lessened in HG-treated H9c2 cells, and rutaecarpine improved the HG-induced injury in H9c2 cells through promoting the autophagy.

When autophagy activity exceeded a certain limit, excessive protein and organelles would be removed, which would accelerate cell death and promote the process of cardiac fibrosis and heart failure (29). Autophagy and apoptosis are necessary to maintain normal survival of the body, and are related to diabetes, cardiovascular disease and other diseases and inflammation (30, 31). Study has shown that there is an obvious relationship between autophagy and apoptosis (32). In DCM mouse model, curcumin stimulated autophagy through JNK1 and AMPK pathways and inhibits cardiac cell apoptosis (33). The autophagy level of rat cardiomyocyte H9c2 decreased and apoptosis increased under the stimulation of high glucose and high lipid, while the addition of autophagy agonist increased autophagy and reduced myocardial cell apoptosis (34).

Here, the apoptosis was increased and autophagy was decreased in H9c2 cells induced by HG. After rutaecarpine treatment for HG-induced H9c2 cells, autophagy was exacerbated and apoptosis was obstructed, which were in line with above studies.

The expression of TRPV1 and autophagy markers in diabetic hearts is decreased (35). TRPV1 activation induces autophagy of ox-LDL-treated vascular smooth muscle cells to prevent foam cells from forming (36). Rutaecarpine promoted NO synthesis and eNOS phosphorylation through activating TRPV1 (37). TRPV1 was related to the expression and release of calcitonin gene-related peptide stimulated by rutaecarpine (38). Rutaecarpine alleviated endothelial injury and gap junction dysfunction induced by Ox-LDL *in vitro* through activation of TRPV1 (39). Blocking TRPV1-dependent autophagy could alleviate nitrogen mustard-caused cutaneous injury (40). Previous studies have indicated that TRPV1-mediated autophagy could also regulate cell apoptosis and oxidative stress (14, 15). Here, we found that TRPV1 expression was declined in H9c2 cells exposed to HG, which could be promoted following rutaecarpine treatment. Additionally, TRPV1 inhibitor hindered the autophagy, resulted in enhanced apoptosis and oxidative stress.

## Conclusion

In conclusion, rutaecarpine exerted no impact on H9c2 cell viability, and could promote TRPV1-mediated autophagy to improve viability and suppress apoptosis and oxidative stress of HG-induced H9c2 cells. However, the effect of rutaecarpine on HG-induced H9c2 cells could be alleviated by inhibition of TRPV1. In our future study, more cell lines from rats or human and further animal studies will be investigated to support the findings. Furthermore, the role of TRPV1-mediated calcium signaling in HG-induced apoptosis, the expression of LC3 and oxidative stress-related proteins will be examined. In addition, HG decreased TRPV1 expression and gain-of-function strategy will be conducted.

## References

1. Yang YY, Chen WY, Sun XT et al. Shexiang baixin pill protects cardiomyocytes against high glucose-induced injury by inhibiting the p38 MAPK and NF- $\kappa$ B pathway. *Chinese J Clin Anat* 2016; 34: 517–527.
2. Murtaza G, Virk HUH, Khalid M et al. Diabetic cardiomyopathy – A comprehensive updated review. *Prog Cardiovasc Dis* 2019; 62: 315–326.
3. Paolillo S, Marsico F, Prastaro M et al. Diabetic Cardiomyopathy: Definition, Diagnosis, and Therapeutic Implications. *Heart Fail Clin* 2019; 15: 341–347.
4. Jia S, Hu C. Pharmacological effects of rutaecarpine as a cardiovascular protective agent. *Molecules* 2010; 15: 1873–1881.
5. Kobayashi Y, Hoshikuma K, Nakano Y, Yokoo Y and Kamiya T. The positive inotropic and chronotropic effects of evodiamine and rutaecarpine, indoloquinazoline alkaloids isolated from the fruits of *Evodia rutaecarpa*, on the guinea-pig isolated right atria: possible involvement of vanilloid receptors. *Planta Med* 2001; 67: 244–248.
6. Moon TC, Murakami M, Kudo I et al. A new class of COX-2 inhibitor, rutaecarpine from *Evodia rutaecarpa*. *Inflamm Res* 1999; 48: 621–625.

7. Zeng SY, Yang L, Lu HQ, Yan QJ, Gao L, Qin XP. Rutaecarpine prevents hypertensive cardiac hypertrophy involving the inhibition of Nox4-ROS-ADAM17 pathway. *J Cell Mol Med* 2019; 23: 4196–4207.
8. Li WQ, Li XH, Du J et al. Rutaecarpine attenuates hypoxia-induced right ventricular remodeling in rats. *Naunyn Schmiedebergs Arch Pharmacol* 2016; 389: 757–767.
9. Xiong Y, Wang HX, Yan H et al. Rutaecarpine Prevents High Glucose-Induced Endothelial Cell Senescence Through Transient Receptor Potential Vanilloid Subtype 1/ SIRT1 Pathway. *J Cardiovasc Pharmacol* 2022; 79: e129–e137.
10. Song XM, Li BJ, Zhang YY et al. Rutaecarpine enhances the anti-diabetic activity and hepatic distribution of metformin via up-regulation of Oct1 in diabetic rats. *Xenobiotica* 2021; 51: 818–830.
11. Peng J, Li YJ. The vanilloid receptor TRPV1: role in cardiovascular and gastrointestinal protection. *Eur J Pharmacol* 2010; 627: 1–7.
12. Amantini C, Mosca M, Lucciarini R et al. Distinct thymocyte subsets express the vanilloid receptor VR1 that mediates capsaicin-induced apoptotic cell death. *Cell Death Differ* 2004; 11: 1342–1356.
13. Wei J, Lin J, Zhang J et al. TRPV1 activation mitigates hypoxic injury in mouse cardiomyocytes by inducing autophagy through the AMPK signaling pathway. *Am J Physiol Cell Physiol* 2020; 318: C1018–c1029.
14. Luo J, Chen J, Yang C et al. 6-Gingerol protects against cerebral ischemia/reperfusion injury by inhibiting NLRP3 inflammasome and apoptosis via TRPV1 /FAF1 complex dissociation-mediated autophagy. *International Immunopharmacol* 2021; 100: 108146.
15. Huang T, Lin Y, Pang Q, Shen W, Chen X, Tu F. The Synergistic Effect of TRPV1 on Oxidative Stress-Induced Autophagy and Apoptosis in Microglia. *Analytical cellular pathology (Amsterdam)* 2021: 7955791.
16. Bao MH, Dai W, Li YJ, Hu CP. Rutaecarpine prevents hypoxia-reoxygenation-induced myocardial cell apoptosis via inhibition of NADPH oxidases. *Can J Physiol Pharmacol* 2011; 89: 177–186.
17. Li JZ, Peng J, Xiao L et al. Reversal of isoprenaline-induced cardiac remodeling by rutaecarpine via stimulation of calcitonin gene-related peptide production. *Can J Physiol Pharmacol* 2010; 88: 949–959.
18. Surbala L, Singh CB, Devi RV, Singh OJ. Rutaecarpine exhibits anti-diabetic potential in high fat diet-multiple low dose streptozotocin induced type 2 diabetic mice and in vitro by modulating hepatic glucose homeostasis. *J Pharmacol Sci* 2020; 143: 307–314.
19. Othman AI, El-Sawi MR, El-Missiry MA, Abukhalil MH. Epigallocatechin-3-gallate protects against diabetic cardiomyopathy through modulating the cardiometabolic risk factors, oxidative stress, inflammation, cell death and fibrosis in streptozotocin-nicotinamide-induced diabetic rats. *Biomed Pharmacother* 2017; 94: 362–373.
20. Lin Y, Tang Y, Wang F. The Protective Effect of HIF-1 $\alpha$  in T Lymphocytes on Cardiac Damage in Diabetic Mice. *Ann Clin Lab Sci* 2016; 46: 32–43.
21. Ramírez S, Gómez-Valadés AG, Schneeberger M et al. Mitochondrial Dynamics Mediated by Mitofusin 1 Is Required for POMC Neuron Glucose-Sensing and Insulin Release Control. *Cell Metab* 2017; 25: 1390–1399.e1396.
22. She F, Sun W, Mao JM, Wang X. Calcitonin gene-related peptide gene therapy suppresses reactive oxygen species in the pancreas and prevents mice from autoimmune diabetes. *Sheng Li Xue Bao* 2003; 55: 625–632.
23. Ren ZK, Zhang ZB, Liu YH, Zhang RP, Yang H. Anti-inflammatory and Anti-oxidative Stress Damage of Catechin Gallate on Diabetic Myocardial in C57 Mice. *Chinese J Exp Traditional Med Formulae* 2018; 24: 148–153.
24. Guo R, Zhang Y, Turdi S, Ren J. Adiponectin knockout accentuates high fat diet-induced obesity and cardiac dysfunction: role of autophagy. *Biochim Biophys Acta* 2013; 1832: 1136–1148.
25. Zhao Y, Zhang L, Qiao Y et al. Heme oxygenase-1 prevents cardiac dysfunction in streptozotocin-diabetic mice by reducing inflammation, oxidative stress, apoptosis and enhancing autophagy. *PLoS One* 2013; 8: e75927.
26. Ouimet M, Ediriweera H, Afonso MS et al. microRNA-33 Regulates Macrophage Autophagy in Atherosclerosis. *Arterioscler Thrombosis Vasc Biol* 2017; 37: 1058–1067.
27. Gao W, Zhou Z, Liang B et al. Inhibiting Receptor of Advanced Glycation End Products Attenuates Pressure Overload-Induced Cardiac Dysfunction by Preventing Excessive Autophagy. *Front Physiol* 2018; 9: 1333.
28. Tanida I. Autophagy basics. *Microbiol Immunol* 2011; 55: 1–11.
29. Bravo-San Pedro JM, Kroemer G, Galluzzi L. Autophagy and Mitophagy in Cardiovascular Disease. *Circ Res* 2017; 120: 1812–1824.
30. Zhang WX, He BM, Wu Y, Qiao JF, Peng ZY. Melatonin protects against sepsis-induced cardiac dysfunction by regulating apoptosis and autophagy via activation of SIRT1 in mice. *Life Sci* 2019; 217: 8–15.
31. Ren J, Zhang Y. Targeting Autophagy in Aging and Aging-Related Cardiovascular Diseases. *Trends Pharmacol Sci* 2018; 39: 1064–1076.
32. Luo G, Jian Z, Zhu Y et al. Sirt1 promotes autophagy and inhibits apoptosis to protect cardiomyocytes from hypoxic stress. *Int J Mol Med* 2019; 43: 2033–2043.
33. Yao Q, Ke ZQ, Guo S et al. Curcumin protects against diabetic cardiomyopathy by promoting autophagy and alleviating apoptosis. *J Mol Cell Cardiol* 2018; 124: 26–34.
34. Xu K, Liu XF, Ke ZQ, Yao Q, Guo S, Liu C. Resveratrol Modulates Apoptosis and Autophagy Induced by High Glucose and Palmitate in Cardiac Cells. *Cell Physiol Biochem* 2018; 46: 2031–2040.
35. Tong J, Lai Y, Yao YA et al. Qiliqiangxin Rescues Mouse Cardiac Function by Regulating AGTR1/TRPV1-Mediated Autophagy in STZ-Induced Diabetes Mellitus. *Cell Physiol Biochem* 2018; 47: 1365–1376.
36. Li BH, Yin YW, Liu Y et al. TRPV1 activation impedes foam cell formation by inducing autophagy in oxLDL-treated vascular smooth muscle cells. *Cell Death Dis* 2014; 5: e1182.
37. Lee GH, Kim CY, Zheng C et al. Rutaecarpine Increases Nitric Oxide Synthesis via eNOS Phosphorylation by TRPV1-Dependent CaMKII and CaMKK $\beta$ /AMPK Signaling Pathway in Human Endothelial Cells. *Int J Mol Sci* 2021; 22: 9407.
38. Yang Y, Chen Q, Jia S et al. Involvement of TRPV1 in the expression and release of calcitonin gene-related peptide induced by rutaecarpine. *Mol Med Rep* 2018; 17: 5168–5174.
39. Peng WJ, Liu Y, Yu YR et al. Rutaecarpine prevented dysfunction of endothelial gap junction induced by Ox-LDL via activation of TRPV1. *Eur J Pharmacol* 2015; 756: 8–14.
40. Chen M, Dong X, Deng H et al. Targeting TRPV1-mediated autophagy attenuates nitrogen mustard-induced dermal toxicity. *Signal Transduct Target Ther* 2021; 6: 29.

Received March 2, 2023.

Accepted April 16, 2023.